# Optimizing chaotic signals for complex radar targets

T. L. Carroll[1,*]

[1] *US Naval Research Lab, Washington, DC 20375*

(Dated: February 9, 2007)

## Abstract

There has been interest in the use of chaotic signals for radar, but most researchers consider only a few chaotic systems and how these signals perform for the detection of point targets. The range of possible chaotic signals is far greater than what most of these researchers consider, so to demonstrate this, I use a chaotic map whose parameters may be adjusted by a numerical optimization routine, producing different chaotic signals that are optimized for different situations. It is also suggested that any advantage for chaotic signals may come in the detection of complex targets, not point targets, and I compare the performance of chaotic signals to a standard radar signal, the linear frequency modulated chirp.

*Electronic address: Thomas.L.Carroll@nrl.navy.mil

**Radar and sonar are used to detect remote objects by transmitting a signal and detecting the reflection of the signal from the target object. When radar and sonar were first developed, signals were generated by analog oscillators, so the signals used in radar or sonar were either periodic signals or sinusoidal signals in which the frequency was swept. Noise signals from analog noise sources were also used. The development of fast digital to analog convertors and fast computers has recently allowed digital synthesis to be used for generating radar and sonar signals, but much conventional wisdom gained from experience with periodic or noise signals must be reconsidered.**

**In this paper, a chaotic map with adjustable parameters is used to generate radar signals. Digital synthesis techniques allow a radar engineer to generate any signal that they can imagine, so the advantage of chaotic systems is not in the chaotic signals themselves, but in the ease with which complex, broad band signals may be designed. Broad band signals are desirable for radar because they allow the determination of distance with greater resolution. Chaotic signals are sometimes described as being noiselike, but it is shown in this paper that for radar applications, chaos is not noise, so known results that hold for noise signals may not be true for chaotic signals.**

**Most radar theory concerns the detection of point targets in Gaussian noise. In this work, the parameters of a chaotic map are optimized to match the chaotic signal to a complex target consisting of several point scatterers, a problem which does not have a simple solution. To make the simulations more realistic, interference from other scatterers is included. This interference is known as clutter, and there is no general theory for a complex target in clutter.**

## I. INTRODUCTION

In the fields of radar and sonar, transmitted signals that are reflected from objects are used to determine the distance to and radial velocity of those objects [**?** ]. Usually, periodic signals or combinations of periodic signals have been used for these applications, but other types of signals such as noise or chaos have also been explored. Chaotic signals may have a large bandwidth, which is useful in increasing the precision with which distances may be

measured. To understand this principle, think of a pulse or a wave packet: the more the wave packet is localized in time, the greater the spread of frequencies used to create the wave packet The application of chaos to radar or sonar has been considered by several groups [**?** **?** **?** **?** **?** **?** **?** **?** ]. To measure distance in radar, one actually measures a delay time, so signals with broader bandwidths increase the precision with which distance may be measured.

Modern digital-to-analog converters have become fast enough to allow for the digital synthesis of some radar signals, which means that any signal that can be described can by synthesized. In this regard, there is nothing unique about chaotic signals applied to radar, as radar engineers can design any signal that they want. The advantages of chaotic systems are in signal design- chaotic systems naturally generate broad band signals. This paper will focus on using a simple chaotic system to design a variety of different radar signals.

The theory of using radar for detecting point objects in Gaussian noise is well known[**?** ], but less is known about complex objects, which contain multiple scattering centers. Non-Gaussian noise also causes problems, as does clutter, which is any reflection from objects other than the target. For these reasons, the chaotic systems below will be used to design radar signals which are matched to complex targets in the presence of clutter.

There has been work on the linear optimization of radar signals to improve signal detection in non-Gaussian noise, or to match the signal to a particular target for target identification[**?** **?** ] . Since I am using a nonlinear chaotic system to generate signals, I must use numerical optimization to vary the parameters of the chaotic system to optimize the chaotic signal for specific applications. The idea of using optimization to improve chaotic signals for certain applications was first suggested by Homer et al[**?** ]. The structure of the particular chaotic system that I use is arbitrary, and many other structures are possible.

## II. RADAR AND SONAR BASICS

### A. Ambiguity Functions

The ambiguity function is a standard measure of a radar signal[**?** ] . The ambiguity function shows the probability of detecting a target on a 2 dimensional plot, where one axis is delay time (distance) and the other axis is Doppler shift (radial velocity). The true target location is plotted at the origin. The ambiguity function shows the range and Doppler

resolution of a radar signal for a point target, and reveals any range-Doppler coupling, or any range ambiguities[**?** ]. Ambiguity in the range can be caused by a periodic signal, for example, in which case distances that are different by 1 signal wavelength appear to be the same distance, and range-Doppler coupling means that it is impossible to distinguish a stationary target at one location from a moving target at a different location.

In the work described below, complex targets are considered, clutter (interference from other targets) is present, and we are interested in ability of the radar signal to highlight one target over another, which is not shown in the ambiguity function. Nevertheless, the ambiguity functions are plotted to give some idea of the nature of the chaotic signals.

### B. Broadband Ambiguity

The range to the target as a function of time is $R(t) = R_0 + v_r t$ , where $R_0$ is the initial range and $v_r$ is the radial component of the velocity. Assuming the target velocity is much slower than the signal velocity (true for radar), the transmitted signal at time $t_1$ then travels a total path length of $2R(t_1)$ , for a phase change of $4\pi R(t_1)/\lambda$ , where $\lambda$ is the wavelength. The Doppler frequency is the derivative with respect to time of this phase shift, which may be simplified to yield

$$f_d = \frac{2f}{c} v_r \tag{1}$$

where $f$is the signal frequency, $f_d$ is the resulting Doppler frequency, and $c$ is the signal velocity. Eq. **??** shows that if the transmitted signal contains many frequencies, then there will also be many Doppler frequencies[**?** ] .

The ambiguity function is defined as

$$\left|\chi(T_R, f_d)\right|^2 = \left| \int_{-\infty}^{\infty} s_t(t) s_t^*(t + T_R) e^{2\pi j f_d t} dt \right|^2 \tag{2}$$

where $s(t)$ is the signal under consideration and $T_R$ is a time delay. The ambiguity function looks like the autocorrelation function for the signal $s(t)$, except for the presence of the exponential term, which shifts all the frequencies in $s^*(t + T_R)$ by the amount $f_d$ . For a fixed Doppler frequency $f_d$ , the ambiguity function is the cross correlation between the signal $s(t)$ and its frequency shifted version.

For a narrow band signal, a single Doppler frequency $f_d$ may be used in eq. **??**, but for a broad band signal, a band of frequencies defined by eq. **??** is necessary [**?** **?** ]. To actually calculate the ambiguity function, the signal $s(t)$ is expanded or compressed along the time axis to simulate a Doppler shifted version of $s(t)$, which will be called $s_d(t)$. We are working with digitized signals, so the discreet version of eq. **??** is calculated, with $s_d^*(t+T_R)$ replacing $s_t^*\left(t+T_R\right)e^{2\pi j f_d t}$ in eq. **??**. The frequencies in $s_d^*(t+T_R)$ have been shifted by the time compression or expansion, so the frequency shift from the exponential term is no longer necessary.

An ambiguity diagram, such as those plotted in fig. **??**, shows the probability of detecting a target at a certain range and Doppler shift. Traditionally, the actual target location is at the origin. Large peaks away from the origin cause ambiguity- it is ambiguous whether the peak is from the target at the origin or from some other nearby target, so a desirable ambiguity diagram has all the probability concentrated in one peak near the origin.

If the product of the time length and bandwidth of different signals is the same, then the volume under their ambiguity diagrams is the same[**?** **?** ] . In practice, this means that improving the range resolution of a signal with a fixed time length and bandwidth, which results in a contraction of the central peak of the ambiguity diagram along the range axis, must result in the ambiguity diagram expanding along the Doppler axis, making the Doppler resolution worse. Improving Doppler resolution also results in worse range resolution. In practice, radar engineers may seek to move ambiguity- i.e, they may engineer signals that reduce the probability of false detection in certain parts of the range-Doppler space [**?** **?** ], although this results in increasing the probability of false detection in other parts of the space. In this paper, adaptive chaotic maps will be used to move ambiguity on the ambiguity plot.

Figure **??** shows ambiguity functions for a point target for a chaotic signal defined below (eq. **??**-**??**), a linear frequency modulated (LFM) chirp with the same frequency and time span, and a sine wave frequency modulated with a uniformly distributed noise signal. The LFM chirp is a commonly used radar signal in which the signal frequency is swept continuously in a linear fashion between 2 values. The map that generated the chaotic signal has a largest Lyapunov exponent of 0.097 bits/iteration.

The length of each of the signals in fig. **??** was 8192 samples, and some additional processing was used with each signal before calculating the ambiguity diagram. The finite

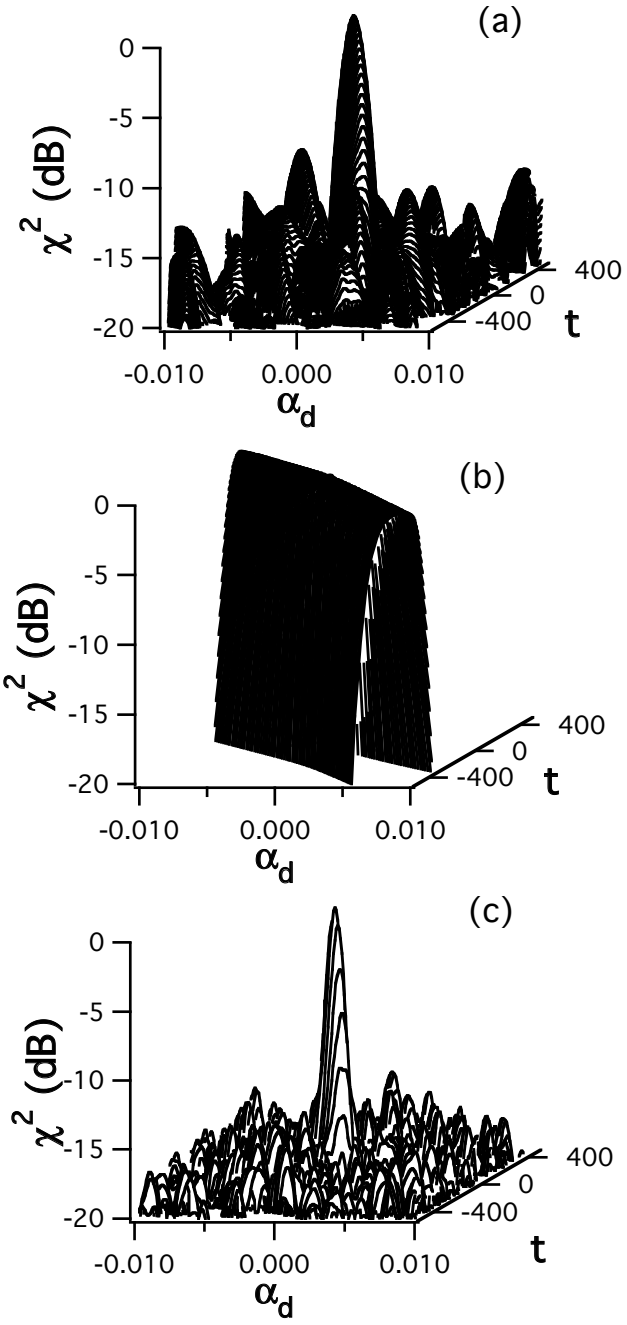


FIG. 1: Ambiguity functions. $\alpha_d$ is the fractional Doppler shift (the amount by which the time axis is expanded), $t$ is the delay in time steps, and $\chi$ is the value of the ambiguity function. The time step in the simulation ws set as 1, so for higher time steps, all factors will be multiplied by the appropriate scaling factor. (a) Ambiguity function for 8192 samples of a chaotic signal described by eqs. **??-??** below. The map that generates the chaotic signal has a largest Lyapunov exponent of 0.097 bits/iteration. (b) Ambiguity function for a linear frequency modulated (LFM) chirp with the same frequency span and length as the chaotic signal in (a). (c) Ambiguity function for a signal frequency modulated by uniformly distributed noise, with the same frequency span and time length as the signals in (a) and (b).

length of these signals imposes an additional modulation of the form of $\sin(x)/x$ on the cross correlation[**?** ] . In order to minimize the finite length effects, each signal is first multiplied by a time window that has an amplitude of 1 in the middle of the signal, and a small amplitude at the ends of the signal. The window in this case is the Blackman window[**?** ], described by $w(t) = 0.42 - 0.5\cos(2\pi t/N) + 0.08\cos(4\pi t/N)$, where $N$ is the number of samples in the signal.

The ambiguity diagram for the chaotic signal has a large central peak, with smaller peaks about 15 dB below the main peak (15 dB is a factor of $10^{1.5}$ ). These side peaks will obscure a small target that is near the main target but whose amplitude is more than 15 dB below the amplitude of the main target. The side peaks are known as sidelobes, and low sidelobes are desirable.

Figure **??**(b) shows the ambiguity diagram for an LFM chirp, which is a commonly used radar signal because of its low sidelobes. The chirp does have a ridge in between the range and Doppler axes, which means that a Doppler shift is not distinguishable from a change in distance.

### C. Chaos vs. Noise

There is a well known result from radar and sonar analysis that states that an LFM chirp signal will have a better signal to noise plus clutter ratio (SINR) in a clutter environment than a noiselike signal[**?** ]. This analysis is based on the properties of the ambiguity diagram. One can consider a group of scatterers distributed with a uniform density over a fixed area (the clutter). The distribution can be along both the range and Doppler axes. A schematic representation of this clutter is shown as the shaded area on fig. **??** (a-b). The amount of interference produced by this clutter will be proportional to the volume that is under the intersection of the ambiguity surface and the scattering area. The ambiguity plot for the LFM chirp (fig **??**(b)) is large only over a small area, so the volume that is also within the scattering area will in general be small, as can be seen in fig. **??**(a); the LFM chirp ambiguity is large only within the diagonal ellipse. The noise ambiguity plot (fig **??**(c)) has a large central peak, surrounded by an area of relatively uniform and non-negligible amplitude, shown as a large circle in fig. **??**(b). From the analysis in Stewart and Westerfield[**?** ], the volume under the intersection of the ambiguity surface and the clutter area is larger for the

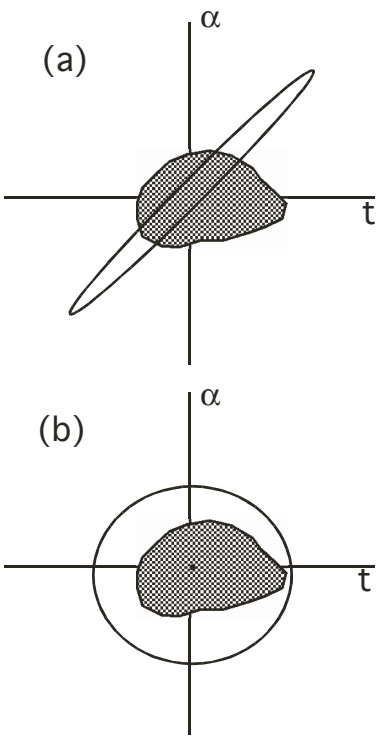


FIG. 2: Schematic representation of the ambiguity plots for an LFM chirp (a) or noise (b) in the presence of clutter (shaded area). $\alpha$ is the Doppler shift axis, and $t$ is the time axis.

noise signal than for the LFM chirp, so the chirp has a higher SINR than the noise signal.

The above analysis does not apply to chaos because chaos is not noise. The ambiguity surface for the chaotic signal in fig. **??**(a) is much less uniform than the ambiguity surface for the noise signal. These nonuniform areas can be moved around by choosing different chaotic signals, so in principle, for a particular set of scatterers, it could be possible for the chaotic signal to have a higher SINR than a chirp signal. One object of this paper is to look for such chaotic signals.

### D. Chaos and Radar

There have been efforts to apply chaotic signals to radar [**?** **?** **?** **?** **?** **?** **?** **?** ]. In most work, only a few well known chaotic systems have been studied, which may give the false impression that there are only a few types of chaotic signals available. Because chaotic systems are nonlinear, there are actually an infinite number of chaotic signals that may be created. One could think of the space of chaotic systems as spanning the range from

periodic deterministic signals to purely random noise. It is true that with modern digital synthesis techniques, any desired signal can be synthesized, and in this respect, there is nothing special about chaotic signals; all the usual laws of signal processing still apply to these broad band signals. An advantage of chaotic systems may be not in the actual signals produced, but in the ease with which broad band signals may be designed and synthesized. Chaotic systems are naturally broad band, and their autocorrelation functions approach zero after some time, so chaos may be a simple and natural way to produce high resolution radar (or sonar) signals.

## III. ADAPTIVE SIGNALS

There has been some work on designing chaotic signals to have specific properties [**?** **?** ], but there are no tools that will fit all situations. Homer et al[**?** ] defined a nonlinear map with adjustable parameters, and used a minimization routine to optimize the map parameters for creating different chaotic communications signals. Taking their lead, I define a simple nonlinear map with adjustable parameters and vary the parameters to optimize the resulting chaotic signal for different radar situations . The chaotic signals were optimized for 2 different situations; first the maps were optimized to increase the returned signal from one complex target compared to a different, nearby target; second, the chaotic signal was optimized to improve the signal to noise plus interference ratio (SINR) for a complex target in spatially extended clutter. It seems likely that any advantage from a chaotic signal will be found when looking at complex targets- in numerical experiments, no advantage with point targets was seen.

Callegari et al [**?** ] have shown that in situations where they can design a chaotic signal to have specific autocorrelation properties, chaos performs at least as well as random noise, so I compare optimized chaotic signals to uniformly distributed random noise signals, to see if there is any advantage in using optimized chaotic signals.

There are other approaches to optimizing radar signals. Pillai et al[**?** ] designed optimal pairs of transmit pulses and receiver filters to optimize the output signal to interference plus noise ratio (SINR) in the presence of colored noise and signal dependant interference. Bergin et al[**?** ] started with linear frequency modulated (LFM) chirp signals and optimized the signal to maximize the SINR in colored noise.

### A. Chaotic Map

The chaotic map that was used for optimization was

$$\begin{aligned} x_{j+1}(1) &= \sum_{i=2}^{N} p(i)\, x_j(i) \bmod 1 \\ x_{j+1}(i) &= x_j(i+1)\; i = 2, 3 \ldots N-1 \\ x_{j+1}(N) &= x_j(1) \\ \xi(j) &= x_j(1) + 0.5 j = 1, 2 \ldots M \end{aligned} \tag{3}$$

where the $p(i)$s where parameters to be optimized. The $x_j$s are real numbers; otherwise, this map bears a strong resemblance to a shift register. For the real numbers, the mod 1 operation means divide by 1 and keep only the remainder. The modulus operation keeps the map output between 0 and 1, and provides the nonlinear element necessary to produce chaos.

The map dimension $N$ was set to 6, resulting in $N-1=5$ parameters to be optimized. For each iteration of the map, designated by an increasing index $j$, the output signal $\xi(j)$ is set equal to $x_n(1)+0.5$. The range of $x_n(1)$ was 0 to 1, so the range of $\xi(j)$ was 0.5 to 1.5 The total number of output samples $M$ was at least 400. The map was started with random initial conditions and iterated 4000 times to allow transients to die out.

It was necessary to convert the discrete map output to a continuous signal so that it could be transmitted. For radar, it is also desirable for the signal to have a constant envelope, because the power amplifier used to transmit the signal works more efficiently with a constant envelope signal. The method used here was similar to a method used by Baranovski[**?** ], where the map output determined the parameters for a defined basis signal. In this case, the basis signal was a single cycle of a sine wave with an amplitude of 1 and a frequency determined by $\xi(j)$. The $j$th cycle of the output signal $s_t(i)$ was

$$s_t(t) = \sin\left(2\pi t / \left[20\xi(j)\right]\right)\; t = 0, 1 \ldots, t < 20\xi(j) \tag{4}$$

The total number of samples for $s_t$ was 1024. The number of samples per cycle of $s_t$ varied from 10 to 30, so the number of cycles for $s_t$ varied, but the average number of cycles was near 50.

Chaotic signals never repeat, so any advantage from using chaos should come when long signals are used. In this paper, 10 pulses of 1024 samples each are used, with each pulse

being created from a different piece of the chaotic trajectory. Because each pulse is different, the actual reflected pulses are not averaged together. Rather, a reference copy of each transmitted pulse is saved and cross correlated with the reflected pulse. The cross correlation $R^2(x, y, \tau)$ for 2 zero mean digitized signals $x(j)$ and $y(j)$ was calculated according to

$$R^2(x, y, \tau) = \frac{\left[\sum_{j=0}^{N} x(j)\, y(j-\tau)\right]^2}{\sum_{j=0}^{N} x(j) \sum_{j=0}^{N} y(j)} \tag{5}$$

where $\tau$ is a discreet time. In addition, a Blackman window (as described above) was applied to the reference signal. The cross correlation of each reflected pulse with its reference copy were then be averaged together. An alternative procedure would be to send a single longer pulse.

When it was desired to compare the result from the optimized map to the result that would be obtained with a noise signal, a random noise signal was substituted for $\xi(t)$ in eq. **??**. The noise signal could have a uniform distribution or a Gaussian distribution, but in the situations studied here, the uniformly distributed noise was found to give better performance.

The parameters $p(i)$ were varied by a downhill simplex algorithm[**?** ]. The optimizations in this paper were all nonlinear, so the optimization routines had many local minima, some with roughly equivalent magnitudes. The local minimum problem might be addressed with a simulated annealing algorithm, but computational issues are not addressed in this paper.

### B. Complex Targets

Radar targets are rarely simple point objects. Complex targets produce a number of reflections with different amplitudes and delays- a process that may be simulated with an finite impulse response (FIR) filter. The question for this section is whether a chaotic signal may be optimized to produce larger returns from a specific complex object.

The simulated targets were made up of 10 reflections with amplitudes randomly chosen from a uniform distribution between 0 and 1, and delays randomly chosen from a uniform distribution between 0 and 200. The signal reflected from the $k$th target was $y_{Tk}(t)$

$$y_{Tk}(t) = \sum_{i=0}^{N_T} a_{Tk}(i)\, s_t(t + \tau_{Tk}(i)) \tag{6}$$

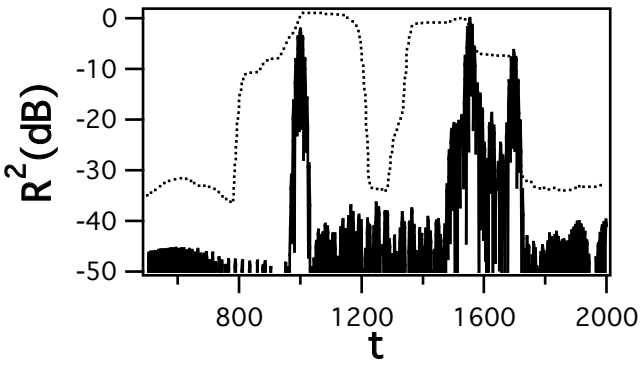


FIG. 3: Cross correlation between transmitted and reflected signals for the complex targets of eq. **??**. Dotted lines are a 200 point running average of the cross correlation.

where $N_\tau = 10$, $a_{Tk}(i)$ was the reflection amplitude, and $\tau_{Tk}(i)$ was the delay.

As a test of the selectivity of a chaotic signal, two different complex targets located at different positions were simulated. The target signals $y_{T1}(t)$ and $y_{T2}(t)$ were both normalized to have an rms amplitude of 1. The total reflected signal from the 2 targets was

$$\psi(t) = y_{T1}\,(t + 1000) + y_{T2}\,(t + 1500) \tag{7}$$

The first thousand samples of the reflected signal $\psi(t)$ were 0, and the end of $\psi(t)$ was padded with zeros so that it had a total length of 8192 samples. In order to show a comparison to a well known radar signal, an LFM chirp signal $c(t)$ was first substituted for the chaotic map signal $s_t(t)$ in eq. **??**, and the targets were detected by cross correlating $c(t)$ with the resulting reflection $\psi(t)$ to produce $R^2(\psi, c_t, \tau)$, which is plotted in Figure **??**. The targets do not produce single peaks because they contain multiple reflections.

Also plotted in fig. **??** is a 200 point running average of $R^2(\psi, c_t, \tau)$. The running average (also known as the integrated reflection power) gives a better indication of the total power actually reflected from the complex target, so in this work, the running average will be used to detect targets. The use of the running average places a limit on the range resolution of the signal.

### C. Optimizing Ratio of One Target to Another

The object of this section is to match a chaotic signal to the target. I assume that I do not have a model of the target available, only the signal reflected from the target. The chaotic

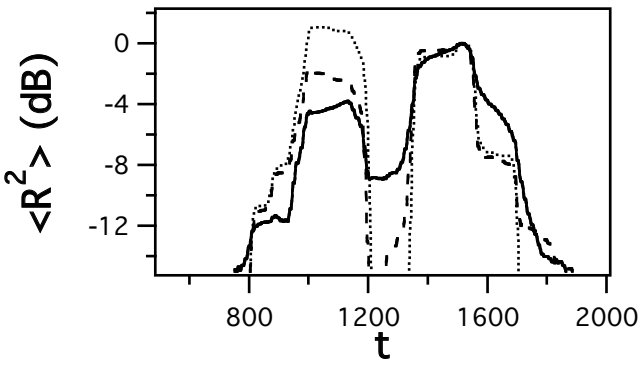


FIG. 4: Optimizing for peak 2/peak 1 ratio. The solid line is the 200 point running average of the radar cross correlation $R^2$ for 2 complex targets when when the chaotic map is optimized for target 2. The dashed line is the running average when a uniformly distributed random noise signal is used in place of the chaotic signal $\xi(t)$ in eq. **??**, and the dotted line is the running average for an LFM chirp. All data is normalized so that the height of peak 2 is 0 dB.

map of eq. **??**-**??** was first optimized to maximize the ratio of the integrated reflection power from target 2 to the power reflected from target 1. In the minimization algorithm, range sidelobes of the cross correlation function were also minimized; otherwise, the minimization routine tended to produce periodic signals rather than chaotic signals. Figure **??** shows a 200 point running average of $R^2(\psi, s_t, \tau)$ when the parameters of the chaotic map were optimized for target 2. The dashed line on fig. **??** shows a running average of the cross correlation when the map signal $\xi(t)$ is replaced by a uniformly distributed random noise signal, while the dotted line shows a running average for an LFM chirp. All averages are normalized so that the amplitude of peak 2 is 0 dB.

The relative heights of the integrated reflection power peaks for the 2 targets depend on the signal that is used. The ratio of peak 2 height to peak 1 height when the optimized chaotic signal is used is greater by 2.2 dB than when the random noise signal is used, and by 4.9 dB compared to when the LFM chirp is used, so the optimization has caused the chaotic signal to be better matched to target 2.

The chaotic map may also be optimized for target 1. Figure **??** shows the result for target 1 optimization. Again, all curves are normalized so that the amplitude of peak 2 is 0 dB. The 200 point running average of the cross correlation when a chaotic signal optimized for peak 1 is used is shown as a solid line. The average for the noise signal is shown by a

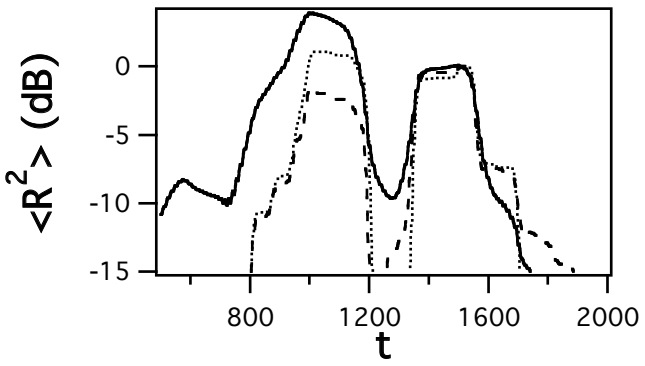


FIG. 5: Optimizing for the peak 1/peak 2 ratio. The dashed line is the 200 point running average of the radar cross correlation $R^2$ for 2 complex targets when a uniformly distributed random noise signal is used in place of the chaotic signal $\xi(t)$ in eq. **??**. The solid line is the running average when the chaotic map is optimized for target 1, while the dotted line is the result for an LFM chirp.

dashed line, while the average for the chirp is shown by a dotted line. When a chaotic signal optimized for the ratio of peak 1 to peak 2 is used, the ratio is greater by 5.5 dB compared to when a random signal is used, and greater by 2.7 dB compared to an LFM chirp.

### D. Transmitting a Target Neutral Signal

Before the advent of high speed digital circuits, radars were analog, so the reference signal was a copy of the transmitted signal that was delayed by an analog delay line. With high speed circuits and digital memories, there is no reason that the transmitted signal and the reference signal have to be identical. In this section, I transmit a target-neutral chaotic signal, which is not optimized for any specific target. The reflected signal from the target is cross correlated with a reference signal that is optimized for a specific target.

The immediate practical advantage of this approach is that I have 1 signal that I transmit for any target. I only need transmit this signal once, and then I can optimize for a specific target offline. I can also compare the reflected signal to reference signals that have been optimized ahead of time for specific targets, allowing me to identify known targets.

In Figure **??**, a target neutral chaotic signal was transmitted, and the reference signal was optimized to maximize the amplitude of the ratio of the peak for target 2/target 1. The

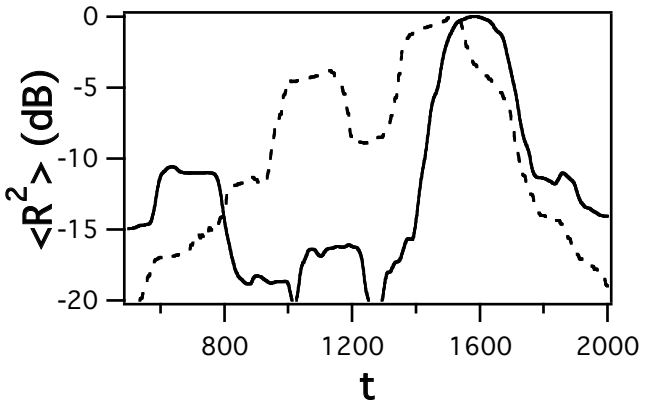


FIG. 6: Running average of the cross correlation $R^2$ between the reflected signal $\xi(t)$ and the optimized reference signal $r_t(t)$ when the reference signal is optimized to maximize the ratio of peak 2 to peak 1 (solid line). The use of a reference signal different than the transmitted signal causes a shift in the peak locations. The dashed line shows the result when the reference and transmitted signals were identical optimized chaotic signals.

location of the peaks in fig. **??** has been shifted because the reference does not match the transmitted signal, so this while this method may be useful for indicating the presence of a specific target, it is not as good for a precise range determination.

In fig. **??**, the ratio of peak 2 to peak 1 has been improved by 16 dB compared to when the transmitted and reference signals were optimized but identical. Peak 1 is low enough that the signal to interference plus noise ratio (SINR) is no longer determined by the height of peak 1. Looking at the background peaks, the SINR for peak 2 is now about 10 dB, compared to 4 dB when transmitted and reference signals were identical and optimized, 2 dB when the 2 signals were generated by uniform noise (fig. **??**), and 1 dB for an LFM chirp (also seen in fig. **??**).

Using the same transmitted signal, it is also possible to optimize the reference signal to maximize the ratio of peak 1 to peak 2. Figure **??** shows the result of this optimization.

Once again, the location of the peaks has been shifted. The ratio of peak 1 to peak 2 in fig. **??** is 12 dB, compared to about 4 dB when the transmitted and reference signals were optimized but identical.

The use of nonidentical transmitted and reference signals can highlight the presence of one target over another. This method could be useful for identifying different closely spaced

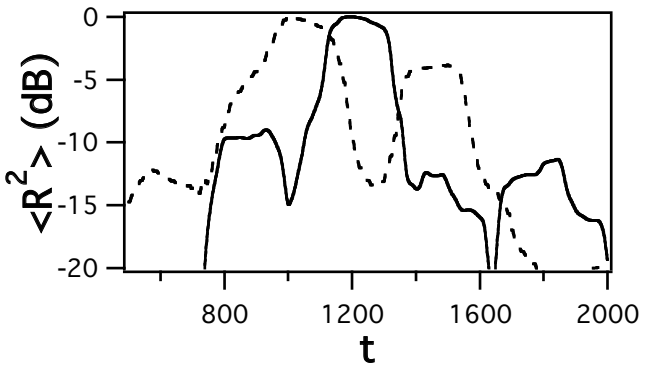


FIG. 7: Running average of the cross correlation $R^2$ between the reflected signal $\xi(t)$ and the optimized reference signal $r_t(t)$ when the reference signal is optimized to maximize the ratio of peak 1 to peak 2 (solid line). The use of a reference signal different than the transmitted signal causes a shift in the peak locations. The dashed line shows the result when the reference and transmitted signals were identical optimized chaotic signals.

targets. There is a complication here; if the target rotates, the FIR filter representation of the target can change, so this method is probably best applied to slowly moving targets.

## IV. TARGET WITH CLUTTER

Detecting a complex target in clutter is similar to the problem of optimizing a signal for a particular target. Clutter in this situation is any object that we are not interested in- it may be a target that is close to the target that we want to detect. If we think of the clutter as just another target, then the problem is similar to the target selection problem discussed above.

### A. Target in Extended Clutter

Clutter caused by scattering from the ground or the sea surface can have a much larger spatial extent than the target. Extended clutter was simulated by adding together 200 reflections of $s_t(t)$ with different amplitudes and delays ranging from 0 to 2000 samples. The reflection amplitudes and delays for the clutter are distributed according to a Gaussian random distribution. As before, the target object contained 10 reflections with delays from 0 to 200 samples, distributed according to a uniform random distribution. The target signal

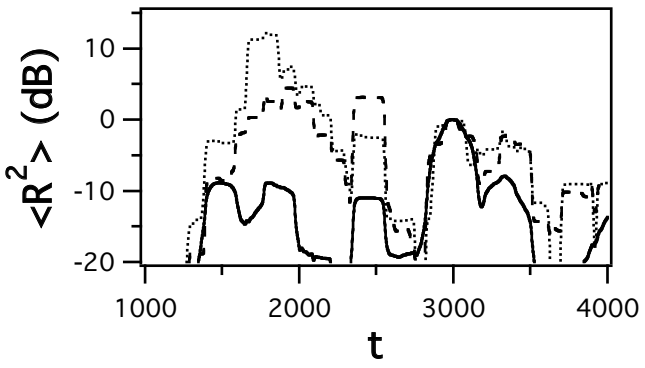


FIG. 8: Optimizing a signal to maximize the return from a complex target (at $t = 2000$) in extended clutter. The solid line is a 200 point running average of the cross correlation for the optimized chaotic signal, the dashed line is for a uniformly distributed noise signal used in place of the chaotic signal, and the dotted line is for an LFM chirp.

$y_{T1}(t)$ and the clutter signal $y_{C1}(t)$ were added to produce the reflected signal

$$\psi(t) = 0.5 y_{T1}(t + 3000) + y_{C1}(t + 2000) \tag{8}$$

Based on the total power in the signal compared to the total power in the clutter signal for the same time period, the signal to interference plus noise ratio (SINR) for $\psi(t)$ was estimated to be 6 dB.

Figure **??** shows a 200 point running average of $R^2(\xi, s_t, \tau)$ in extended clutter when the transmitted and reflected signals were identical. The solid line is for an optimized chaotic signal, the dotted line corresponds to an LFM chirp, and the dashed line is when a uniformly distributed random signal is used in place of the chaotic signal $\xi(t)$ in eq. **??**. All plots were normalized so that the value of the peak at the target location (point 3000) was 0 dB. Optimizing the chaotic signal decreases the average of the cross correlation with clutter reflection and increases the cross correlation with the target reflection. If the SINR is measured by measuring the interference at the highest point in the clutter signal, then the improvement in SINR for the optimized chaotic signal compared to the noise signal is 13 dB, and compared to the LFM chirp the improvement is 21 dB. It is actually not obvious that there is a target reflection in the noise or LFM chirp signals, as the integrated reflected power at the target location is below the clutter level.

The optimized chaotic signal still performs better than the noise or chirp signals if the clutter distribution is uniform, but the differences are not as large. For uniform clutter, the

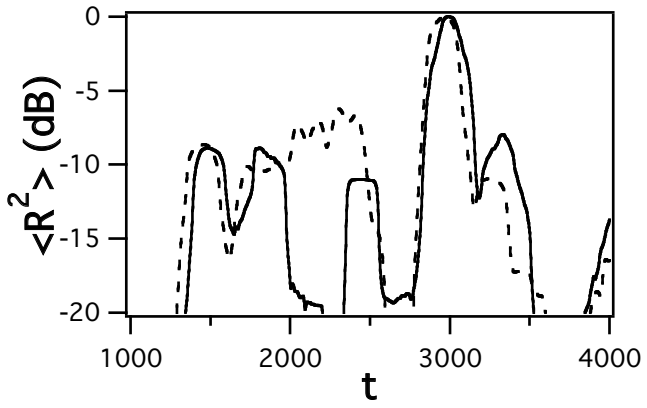


FIG. 9: The solid line is a 200 point running average of the cross correlation $R^2$ for a complex target in extended clutter when the transmitted and reference signals are the same optimized chaotic signal. The dashed line is when a target-neutral signal is transmitted and the reference signal is optimized.

SINR for the optimized chaotic signal is 5.7 dB better than the SINR for the noise signal, and 8.9 dB better than for the LFM chirp signal.

The SINR ratio is actually not as good for this extended clutter when a target-neutral signal is transmitted and the reference signal is optimized. Figure **??** shows the running average of the cross correlations when the reference signal is the same as the transmitted signal, and when it is different.

In fig. **??**, using a target-neutral transmitted signal and optimizing the reference signal yields a SINR that is 2.6 dB worse than when the transmitted and reference signals are the same optimized chaotic signal. The target-neutral signal is still better than the noise or chirp signals in fig. **??**, however, and the same transmitted signal can be used for different targets, so that only the reference signal needs to be optimized.

It reasonable to ask, if a target model is available, why not use that model explicitly, rather than optimize a chaotic signal for the target. In order to test this idea, the signal $s_m(t)$ was generated from a model of the target. The model was generated in the same manner as eq. **??**, by adding copies of the signal $s_t(t)$ with the same delays and amplitudes as used for the target. For this simulation, st(t) was generated by substituting a uniformly distributed noise signal for the chaotic signal $\xi(t)$ in eq. **??**.

The cross correlation was performed in the usual manner, using the target model signal

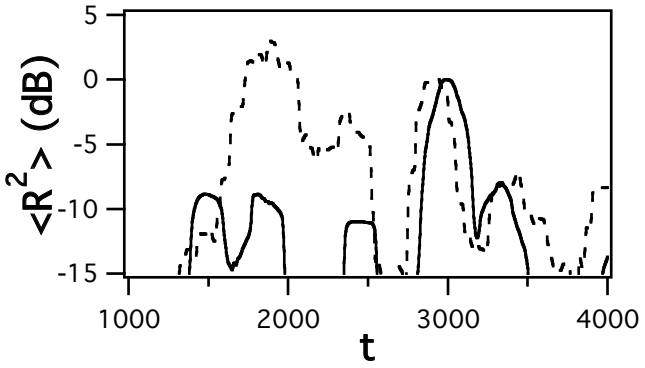


FIG. 10: The solid line is a 200 point running average of $R^2$ for a complex target in extended clutter when the transmitted and reference signals are the same optimized chaotic signal. The dashed line is when a transmitted signal based on uniform noise is used with a reference signal based on an explicit model of the target.

$s_m(t)$ in place of the transmitted signal $s_t(t)$ as a reference. The 200 point running average of the cross correlation is compared to the running average when the transmitted and reference signals are identical optimized chaotic signals in Figure **??**. The optimized chaotic signal still outperforms the model-based signal, with an SINR that is 11 dB better than the model based signal. The model-based signal is well matched to the target, but it does not take the clutter into account. The optimized chaotic signal is optimized to produce the maximum contrast between the target and the clutter.

If the target moves (without rotating), the same optimized chaotic signals can be used, as long as the clutter stays the same. Figure **??** shows a running average of the cross correlation when the target location has changed from 3000 to 2000, but all other signals stayed the same as in fig. **??**.

The SINR for the target is still $> 0$ dB when the target location has moved, as is seen in fig. **??**, but when the target is at $t = 2000$, the SINR when the target-neutral chaotic signal with an optimized reference is used is 3 dB greater than when the transmitted and reference signals are identical

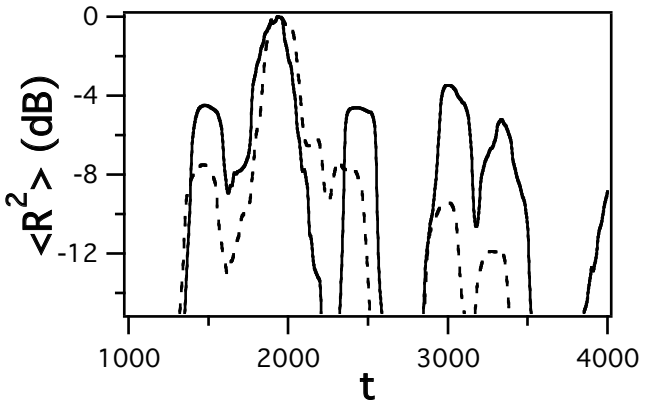


FIG. 11: The solid line is a 200 point running average of $R^2$ for a complex target in extended clutter when the transmitted and reference signals are the same optimized chaotic signal. The dashed line is when a target-neutral signal is transmitted and the reference signal is optimized. The difference between fig. **??** and fig. **??** is that in fig. **??**, the target is at $t = 2000$, while in fig. **??**, the target was at $t = 3000$.

### B. Effects of Ambiguity

The results for the effects of the different signals in clutter may be partly explained by the ambiguity functions of the different signals, and how they interact with the clutter. In the example described above, all of the targets are stationary, so the goal is to maximize the amount of energy returned by the target compared to the amount of energy returned by the clutter for zero Doppler shift. The time and Doppler components of the ambiguity function are not independent; for signals with the same frequency span and time length, the total volume under the ambiguity surface is the same[**?** **?** ]. Figure **??** shows ambiguity functions for scattering from the clutter for the optimized chaotic signal and the noise signal used in fig. **??**.

Figure **??** was computed by comparing the transmitted signal to the signal reflected from the clutter only. The total volume under both ambiguity functions in fig. **??** is the same, but it can be seen that a much larger fraction of the volume for the chaotic signal is at nonzero Doppler shifts. The cross correlation essentially takes a slice through the ambiguity function at constant Doppler, so the optimized chaotic signal reduces the energy returned by the clutter at 0 Doppler, improving the SINR. The chirp signal reflected from the clutter also returns a larger portion of its energy at 0 Doppler shift, but the result is not as obvious

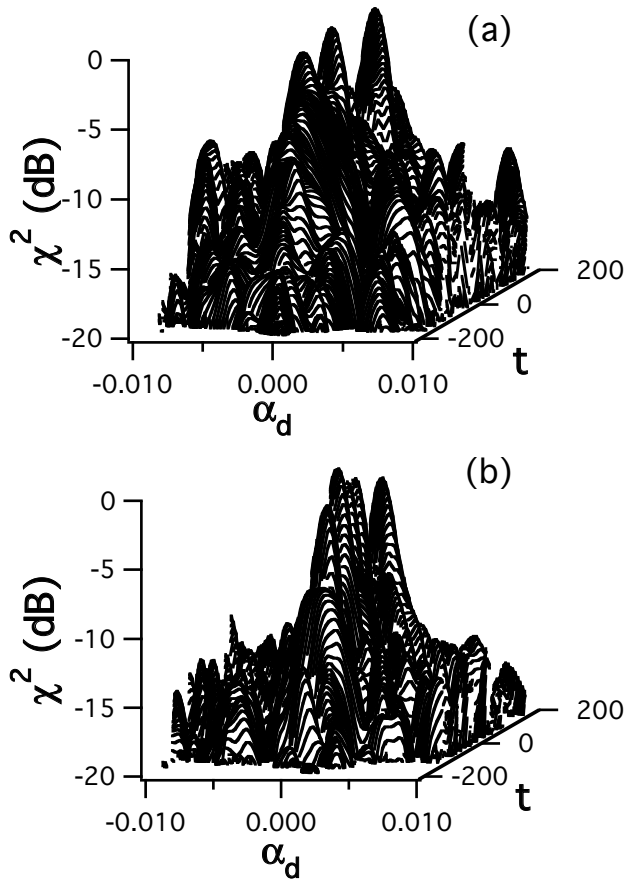


FIG. 12: .Clutter ambiguity function $\chi^2$ for the chaotic signal used in fig. **??**(a) and the noise signal used in fig **??**(b). $\alpha_d$ is the fractional Doppler shift.

from a plot.

To perform a simple comparison of reflected signal power and reflected noise power, the 0 Doppler cross correlations for target only ($R^2(y_T, s_t, \tau)$ ) or clutter only ($R^2(y_C, s_t, \tau)$ were both computed and normalized by the total volume under the corresponding ambiguity functions, $A_T$ or $A_C$. Using this normalization, the integrated value of $R^2(y_T, s_t, \tau)/A_T$ was compared to the integrated value of $R^2(y_C, s_t, \tau)/A_C$ for all 3 signals. For the optimized chaotic signal, the signal power to noise power ratio computed in this way was 1.7; for the noise and chirp signals, this ratio was 1.37. This is only a crude estimate of the actual signal to clutter ratio because the clutter and target reflections cant be separated in this way.

## V. CONCLUSIONS

While the work above leaves some practical questions unanswered, it does show that a simple chaotic system can generate many different chaotic signals, which are useful for different applications. It also seems likely from the work above that chaotic signals are most likely to be useful for complex targets. When studying the application of chaotic signals to radar, it is necessary to consider many more chaotic systems than the few that are usually studied (the Bernoulli shift map, the tent map, the logistic equation, etc.). Outside of a few simple cases, there is as yet no systematic method to design chaotic systems for particular applications. The optimization methods used above have the disadvantage that they are computationally intense and they are slow.

The chaotic map systems I considered here would require digital synthesis, but it has been suggested that one possible advantage of chaotic systems for radar is that one could generate broad band signals with simple analog hardware [**? ? ? ?** ], and microwave chaotic circuits are being developed.

## VI. ACKNOWLEDGEMENTS

I would like to thank Phil Atkins for many useful discussions

---

[] M. I. Skolnik, *Introduction to Radar Systems* (McGraw-Hill, New York, 2001)

[] B. Flores, E. A. Solis and G. Thomas IEEE Proceedings on Radar, Sonar and Navigation **150**, 313-322 (2003)

[] L. Fortuna, M. Frasca and A. Rizzo IEEE Transactions on Instrumentation and Measurement **52**, 1809-1814 (2003)

[] Y. Hara, T. Hara, T. Seo, H. Yanagisawa, P. Ratliff and W. Machowski Proceedings of the 2002 IEEE Radar Conference (IEEE Cat. No.02CH37322) 227-232 (2002)

[] F. Y. Lin and J. M. Liu IEEE Journal of Quantum Electronics **40**, 815-820 (2004) W. Machowski and P. Ratliff Radar 2002 (IEE Conf. Publ. No.490) 474-477 (2002)

[] V. Venkatasubramanian and H. Leung IEEE Signal Processing Letters **12**, 528-531 (2005)

[] P. Willett, J. Reinert and R. Lynch 2004 IEEE Aerospace Conference Proceedings (IEEE Cat. No.04TH8720) 2236-48 Vol.4 (2004)

[] K. A. Lukin Telecommunications and Radio Engineering **55**, 8-16 (2001)

[] P. R. Atkins and A. J. Fenwick Proceedings of the Institute of Acoustics **26**, 154-162 (2004)

[] J. S. Bergin, P. M. Techau, J. E. D. Carlos and J. R. Guerci *IEEE Radar Conference* (IEEE,2005)

[] S. U. Pillai, H. S. Oh, D. C. Youla and J. R. Guerci IEEE Transactions on Information Theory **46**, 577-584 (2000)

[] M. E. Homer, S. J. Hogan, M. d. Bernardo and C. Williams IEEE Transactions on Circuits and Systems II: Express Briefs **51**, 511-516 (2004)

[] P. M. Woodward, *Probability and Information Theory, with Applications to Radar* (Artech House, Dedham, MA, 1980)

[] M. Dawood and R. M. Narayanan IEEE Proceedings on Radar, Sonar and Navigation **150**, 379-386 (2003)

[] K. T. Wong Proceedings of the 1998 IEEE Radar Conference, RADARCON'98. Challenges in Radar Systems and Solutions (Cat. No.98CH36197) 105-110 (1998)

[] A. V. Oppenheim and R. W. Schafer, *Digital Signal Processing* (Prentice-Hall, Englewood Cliffs, 1975)

[] J. L. Stewart and E. C. Westerfield Proceedings of the IRE **47**, 872-881 (1959)

[] S. Callegari, R. Rovatti and G. Setti IEEE Transactions on Circuits and Systems Part I: Fundamental Theory and Applications **50**, 3-15 (2003)

[] A. Tsuneda IEEE Transactions on Circuits and Systems-I Regular Papers **52**, 454-462 (2005)

[] A. L. Baranovski and W. Schwarz IEICE Transactions Fundamentals **E82-A**, 1762-1768 (1999)

[] W. H. Press, B. P. Flannery, S. A. Teukolsky and W. T. Vetterling, *Numerical Recipes* (Cambridge University Press, New York, 1990)

[] S. Hayes, C. Grebogi, E. Ott and A. Mark Physical Review Letters **73**, 1781-1784 (1994)

[] L. Illing and D. J. Gauthier Chaos **16**, 033116 (2006)

[] C. P. Silva and A. M. Young *1998 IEEE International Symposium on Circuits and Systems* 489-493 (IEEE,1998)

[] J. N. Blakely and N. J. Corron Chaos **14**, 1035-1041 (2004)